Investigation of the Structural, Optical and Electrical Properties of $AgInSe_2$ Thin Films

Iman Hameed Khudayer
Bushra Hashem Hussein Ali
Mohammed Hamid Mustafa
Ayser Jumah Ibrahim
Dept. of Physics/ College of Education for Pure Science (Ibn Al-Haitham) / University of Baghdad
demanphd2005@gmail.com
Received in:12/June/2017, Accepted in:2/October/2017

Abstract

The Silver Indium Selenide ($AgInSe_2$) (AIS) thin films of (300 ±20) nm thickness have been prepared from the compound alloys using thermal evaporation technique onto the glass substrate at room temperature, with a deposition rate (3±0.1) nm sec^{-1}.

The structural, optical and electrical properties have been studied at different annealing temperatures (Ta=450, 550 and 650) K.

The amount or (concentration) of the elements (Ag, In, Se) in the prepared alloy was verified using an energy dispersive x-ray spectrometer (EDS) technology. X-ray diffraction analysis shows that AIS alloy prepared as (powder) and the thin films are polycrystalline of tetragonal structure with preferential orientation (112). The crystalline size increases as a function of annealing temperature. The atomic force microscope (AFM) technique was used to examine the topography and estimate the surface roughness, also the average grain size of the films. The results show that the grain size increases with annealing temperature.

The optical band gap of the films lies in the range 1.6-1.9 eV. The films appear to be n-type indicating that the electrons as a dominant charge carrier. The electrical conductivity increases with a corresponding increase in annealing temperature.

Keywords: AIS, Films, Structural, Optical, Electrical conductivity, Hall Effect, Thermal Evaporation.

Introduction

In recent years, considerable efforts have been made to grow device-quality thin films by optimization of growth parameters for applications in optoelectronic devices. The ternary semiconductor compounds with the formula $A^{I}B^{III}C^{VI}_2$ such as $CuAlS_2$, $AgAlSe_2$, etc. have been widely investigated because of their potential applications in electro-optic, the chalcopyrite type crystals the most intensive studies have been carried out in the series of I-III-VI_2 family compounds where Cu is involved as a group I element, very few works have appeared in literature where the group I element is Ag [1].

AIS semiconductors have been produced by several[4]techniques such as: co-evaporation [2,3], ultra-high vacuum pulsed laser deposition [4], horizontal Bridgman method [5], molecular beam epitaxial [6], vertical gradient temperature freezing method [7] and solid state microwave irradiation [8]. In this work, we have prepared Ag-In-Se thin films by thermal evaporation technique, followed by an adequate annealing treatment.

Experimental

The alloy of $AgAlSe_2$ was obtained by fusing the mixture of the appropriate amount of the elements Ag, In and Se of high purity (99.999%) in an evacuating fused quartz ampoules with (2×10^{-3} Torr), heated at (1200 K) for five hours. The films of 300±20 nm thickness were deposited by the thermal evaporation technique at room temperature using the Edward coating unit model (E 306) with molybdenum boat. Energy dispersive x-ray spectrometer (EDS) was used to investigate the amount or (concentration) of the elements (Ag, In, Se) of $AgInSe_2$ alloy.

The crystal structure of the alloy and films was characterized by using X-ray diffraction (XRD) by (Shimadzu6000 X-ray Diffraction) with the copper target of the wavelength (λ=1. 5406) Å. Lattice constants, crystalline size were specified, the inter planar spacing d_{hkl} (Å) between consecutive parallel planes was measured by Bragg's law [9]:

$n\lambda = 2\theta\, d_{hkl} \sin(\theta)$ ..... (1)

Where, n is the order of diffraction and θ is the angle of incidence. The average crystalline size can be estimated using the Scherrer's Formula [10]:

$$C.S = \frac{0.94\lambda_{X-Ray}}{\beta_{(FWHM)}\cos\theta_B} \quad \text{.....(2)}$$

Where, β is the full width at half maximum intensity in radians.

(AFM) was employed to investigate the surface morphology of the $AgInSe_2$ films as a device type of (SPM -AAA3000 contact mode spectrometer, Angstrom). Optical measurement has been constructed using UV-Visible 1800 spectrophotometer.

The thickness (t) of all prepared films was measured by using the weighing method according to the following relation [11]:

$t = m / A.\rho$ ..... (3)

Where; m, ρ, A were the mass, density and area of the films. Using a sensitive balance whose sensitivity of the order (10^{-4}) gm.

The optical absorption spectrum was utilized to define the optical energy gap (E_g^{opt}) eV using Tauc formula [12]:

$\alpha h\nu = B (h\nu - E_g^{opt})^{1/r}$ .....(4)

Where, B is a constant, hν is the photon energy (eV) and r is constant, that it may take values 2, 3, 1/2, 3/2 depending on the material and the type of the optical transition . The absorption coefficient **(α)** value can be computed from the formula [13]:

$$\alpha = 2.303\frac{A}{t} \quad \text{.....(5)}$$

Where, A is the optical absorbance.

The refractive index value can be calculated from the formula [14]:

$$n_o = \left[\frac{4R}{(1-R)^2} - k^2\right]^{\frac{1}{2}} + \left(\frac{1+R}{1-R}\right) \quad \text{.....(6)}$$

where k represents the extinction coefficient, which is calculated by the relation [14]:

$$k = \frac{\alpha\lambda}{4\pi} \quad \text{.....(7)}$$

The real ε_r and imaginary ε_i part of dielectric constant can be calculated by using the following equations [15]:

$$\varepsilon = \varepsilon_r - i\varepsilon_i \quad \text{.....(8)}$$

$$\varepsilon_r = n_0^2 - k_0^2 \quad \text{.....(9)}$$

$$\varepsilon_i = 2n_0k_0 \quad \text{.....(10)}$$

The electrical resistance (R_o) of (AIS) films has been measured as a function of temperature within the range (298-503) K by using Keithly 616 Digital Electrometer and electrical oven, then the resistivity (ρ) has been calculated using the formula [16]:

$$\rho = R_0\frac{b\times t}{L} \quad \text{.....(11)}$$

Where; b is the electrode width and L is the distance between two Al electrodes. The conductivity ($\sigma_{d.c}$) associated with the resistivity as in the equation [16]:

$$\sigma_{d.c} = \frac{1}{\rho} \quad \text{.....(12)}$$

Hall Effect measurements have been managed by Van der Pauw (Ecopia HMS -3000) to determining majority carrier concentrations, type of carrier and their mobility in thin films.

Result and discussion

Energy dispersive x-ray spectrometer (EDS) used to examine the amount or (concentration) of the elements (**Ag, In, Se)** in the alloy. The results are shown in figure (1) and table (1).

Figure (2) shows the XRD pattern of (AIS) bulk powder, which illustrates that the $AgInSe_2$ was a chalcopyrite material in polycrystalline (tetragonal phase) structure as it is compared with the standard values in ICDD cards. The spectrum is considered to exhibit sharp peaks at (112),(200), (220), (204), (312), (116),(400), (316), and (424) corresponding to 2θ values equal to 25.72, 29.45, 41.95, 42.92, 49.84, 51.51, 60.72, 68.42 and 77.12 respectively. The X-ray diffraction parameters inter planar spacing (d), Miller indices and crystalline size for $AgInSe_2$ alloy are listed in table (2), they prefer orientation at (112) planes. Whereas from the X-ray diffraction patterns of $AgInSe_2$ thin films with different annealing temperatures, one can observe that the thin films have the polycrystalline tetragonal structure as shown in figure (3). The figure indicates that the patterns include three sharp peaks referred to (112), (220) and (312) direction. As well, this figure confirms that the preferential orientation is in the (112) direction. The structural parameters of annealed $AgInSe_2$ thin films with different annealing temperatures were illustrated in table (3). The crystallite size has been estimated of the FWHM value of the

(112) peak by using Scherrers equation and is observed, it increased with Ta as shown in table (3). These results were matched with [3,17]. By increasing the Ta the locations of the measured diffraction peaks do not change significantly , but the intensities of the peaks increase. This is due to the improvement of crystalline of the films.

Figure (4) shows the three -dimensional (3D) of $AgInSe_2$ thin films with different Ta. From this figure, it can be deduced that these films have spherical grains granting the smooth surface morphology. The values of surface roughness and the grain sizes are calculated. It has been observed that a surface roughness were equal to (0.608, 0.936,1.65 and 0.809) for different Ta (RT, 450,550 and 650) K respectively. The grain size has been observed (86.68, 90.49, 106.54 and 68.06) for (RT, 450, 550 and 650) K respectively. Therefore, the average diameter of AIS thin film with annealing temperature 550K (see Fig. 4, c) is larger than the AIS thin film (Figure 4, a, b, d).

The absorbance and transmittance spectrum of AIS thin film were evaluated as a function of wavelength at different annealing temperatures as in Figure (5). This figure believed that the absorbance increases in the visible wavelength range as a function of annealing temperature. The behavior of the transmittance spectra is opposite completely to that of the absorbance spectra. From figure (6), we can observe that the α values, which were calculated using equation (4), indeed, own high amount reached above (10^4) cm^{-1}. It was pointed that the α values in general increases as a function of annealing temperature, which is attributed to an increase in absorbance of used films. From table (4) we found that the value of α increases from (5.8-6.6) $\times 10^4 cm^{-1}$ with the increase of Ta. The value of E_g^{opt} decreases (from 1.8 to 1.6) eV and then increases to (1.9) eV with the increase of Ta as shown in table (4) and figure (6). The decrease in the band gap (Eg^{opt}) values may be describable of the increase in defect states near the bands, this result is in agreement with ref. [3].

The Variation of optical constants with photon energy for $AgInSe_2$ thin films at different annealing temperatures is shown in figure (7), such that, refractive index (a) extinction coefficient (b) real (c) and imaginary part of the dielectric constant (d). Table (4) indicates that n valuable decreases with the rise of Ta. This behavior maybe because of the decreasing in the reflection, which the refractive index in turn depends on it. Extinction coefficient (k) in general increment with Ta this is attributed to the same reason mentioned previously in the absorption coefficient, because the behavior of k is similar to α. The variables of ε_r and ε_i versus photon energy at different Ta are shown in figure 8(c & d). The behavior of ε_r is similar to that of the refractive index because of the small value of k^2 compared with n^2, while ε_i behavior is similar to that of extinction coefficient because it mainly depends on the k value, which is related to the variation of absorption coefficient. The variables of ε_r and ε_i with different annealing temperatures film are non -systematic. This means that this material possesses a specialized property with Ta.

We can deduce from the variation of the resistivity verse annealing temperature for all samples of AIS films, that the resistivity values decrease as the Ta rises due to the improvement in the film construction. We believe that there was a reduce in dangling bonds, defects like vacancy sites, and point defect in the film structure, therefore the resistivity of the films decreases from (1.32 Ω.cm to 0.30 Ω.cm) as the Ta increases from (RT to 550 K) as shown in Figure (8), which presented a plot of lnσ versus 10^3 /T for different Ta. From this figure the activation energy can be determined. Electrical conductivity increases as the Ta enlarges because of the rise in the number of available transport charge carriers. We can notice from figure (8) that all AIS films have two mechanisms for electrical conductivity which means that there are two mechanisms of transport of free carriers with two values of the activation energy (E_{a1}, E_{a2}) each one predominating in a different temperature range. The electrical conductivity of these films is affected by the transport of free carriers in extended states beyond the mobility edge at higher temperature ranges (403-473) K, as well

as carriers excited into the localized states at the edge of the band and hopping at other range of temperature (300-393) K [13] as shown in Table (5).

The type of charge carriers, concentration (n) and Hall mobility (μ_H) has been estimated from Hall measurements. These values are listed in Table (6). The negative sign of the Hall coefficient indicates that the conductive nature of the film is n-type, i.e. electrons are the majority charge carriers, this result is in agreement with ref. [18], i.e Hall voltage decreases with the increase of the current. The carrier concentration of the order $10^{17}cm^{-3}$ is in a good agreement with refs [3,19]. We can notice from Table (6) that the carrier concentration and mobility increase with increas of Ta.

Table (1): The composition of $AgAInSe_2$ alloy determined by (EDS)

	Calculated (Wt%)	Test (Wt%)
Ag	28.337	28.188
In	30.162	30.085
Se	41.491	41.38

Table (2): Structural parameters of $AgInSe_2$ alloy

Std.) (Deg.)	**2θ (Exp.) (Deg.)**	**d_{hkl} (Std.) (Å)**	**d_{hkl} (Exp.) (Å)**	hkl
25.726	25.727	3.46	3.45	(112)
29.355	29.45	3.04	3.03	(200)
41.96	41.95	2.151	2.15	(220)
42.97	42.92	2.103	2.105	(204)
49.96	49.84	1.824	1.828	(312)
51.469	51.51	1.774	1.772	(116)
60.808	60.725	1.522	1.523	(400)
68.708	68.42	1.365	1.369	(316)
77.39	77.12	1.232	1.23	(424)

Table (3): Experimental XRD data for $AgInSe_2$ thin films at different Ta.

T (K)		**2θ (Deg.)**	**d_{hkl} (Exp.) (Å)**	**hkl**	**FWHM (Deg.)**	**C.S (nm)**
Ta	RT	25.72	3.458	(112)	0.472	17.127
		41.95	2.15	(220)		
		49.84	1.828	(312)		
	450	25.75	3.455	(112)	0.400	21.277
		41.98	2.14	(220)		
		49.89	1.825	(312)		
	550	25.8	3.449	(112)	0.211	40.336
		42.1	2.143	(220)		
		49.92	1.824	(312)		
	650	25.82	3.446	(112)	0.376	22.637
		42.3	2.134	(220)		

		49.95	1.823	(312)		

Table (4): Optical constant for $AgInSe_2$ thin films at different Ta.

Optical constant at λ=410nm							
Measurement temp.		E_g^{opt} (eV)	$\alpha\times10^4$ $(cm)^{-1}$	n	k	ε_r	ε_i
RT		1.8	5.8	1.34	0.19	1.77	0.51
Ta (K)	450	1.75	6.17	1.24	0.2	1.5	0.54
	550	1.6	6.6	1.2	0.21	1.39	0.51
	650	1.9	4.68	1.61	0.15	2.5	0.36

Table (5): Values of D.C conductivity and activation energies for $AgInSe_2$ thin films at different T_a.

Measurement temp.		**σ $(\Omega.cm)^{-1}$**	**E_{a1} (eV)**	**Tem.range (K)**	**E_{a2} (eV)**	**Tem.range (K)**
RT		0.755	0.043344	300-393	0.17544	403-473
Ta(K)	**450**	1.221403	0.051084	300-393	0.176128	403-473
	550	3.320117	0.052374	300-393	0.178042	403-473
	650	2.013753	0.051417	300-393	0.176022	403-473

Table (6); Hall parameters for $AgIn_xe_2$ thin films at different Ta.

Measurement temp.		**$R_{(H)}$**	**$\mu_H(cm^2/V.S)$**	**n (cm^{-3})**
RT		-22.32	16.85	2.8E+17
Ta(K)	**450**	-12.2549	14.96817	5.1E+17
	550	-7.467145	24.79179	8.37E+17
	650	-9.057971	18.24052	6.9E+17

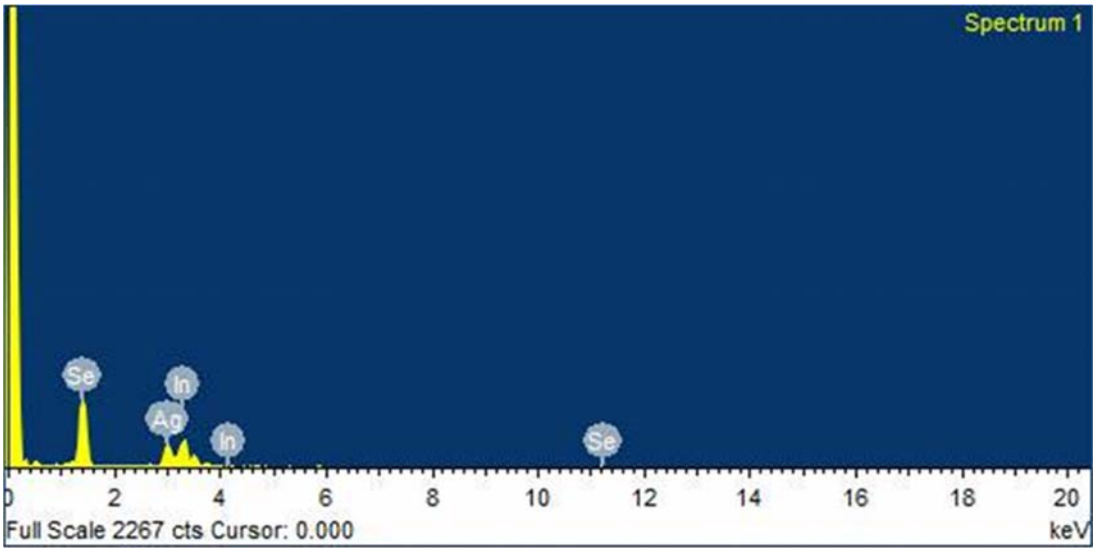

Figure (1): EDS patterns for $AgInSe_2$ alloy.

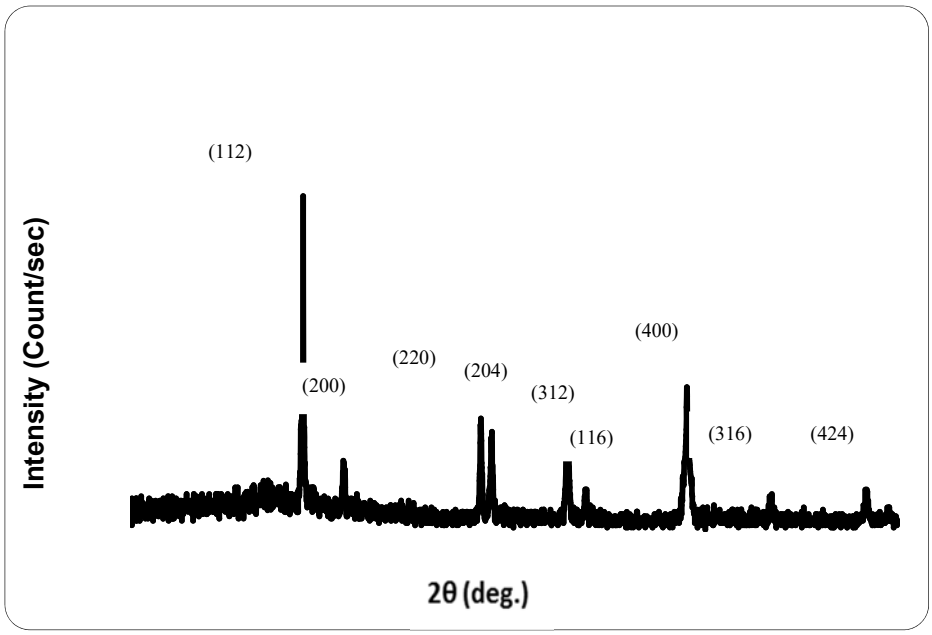

Figure (2): X-ray diffraction pattern of $AgInSe_2$ alloy.

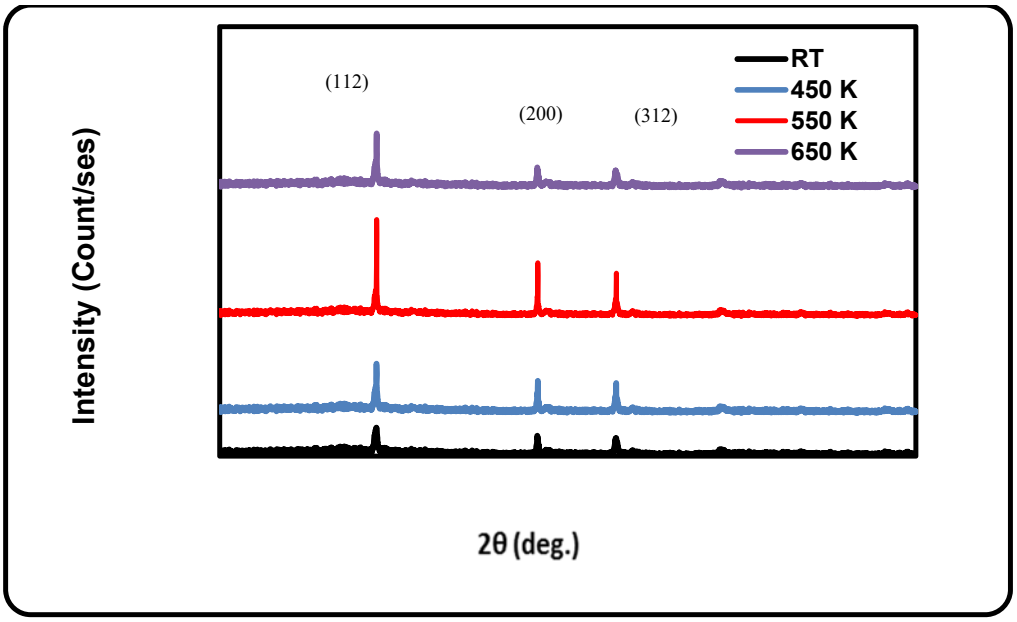

Figure (3): X -ray diffraction pattern of $AgInSe_2$ thin film with a thickness (t=300nm) annealed at different Ta.

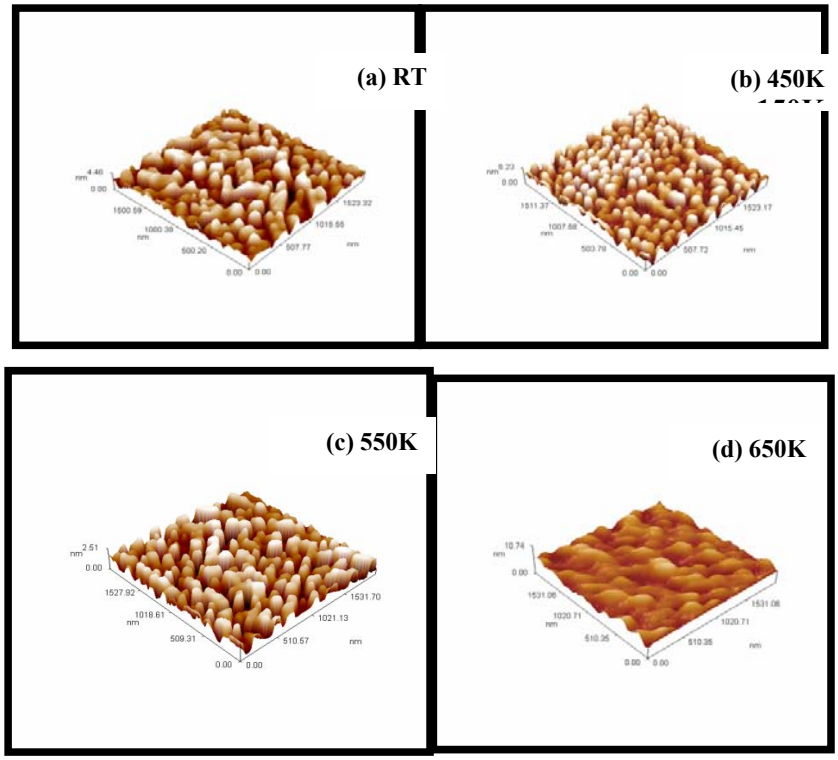

Figure (4): 3D Atomic force microscopy (AFM) of $AgInSe_2$ thin film with a thickness (t=300nm) annealed at different Ta.

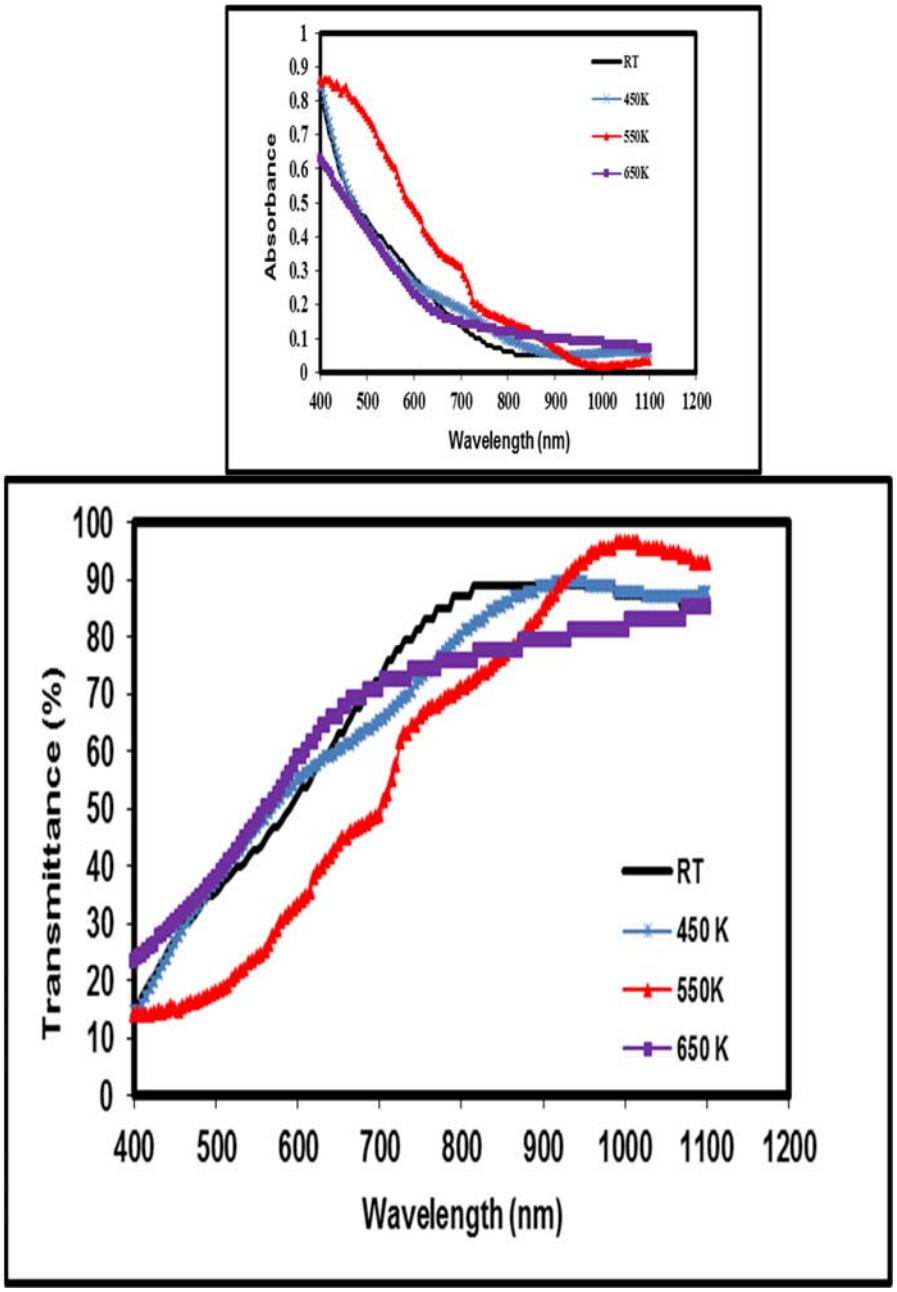

Figure (5): The Absorbance and Transmittance spectrum of $AgInSe_2$ thin film with a thickness (t=300nm) annealed at different Ta.

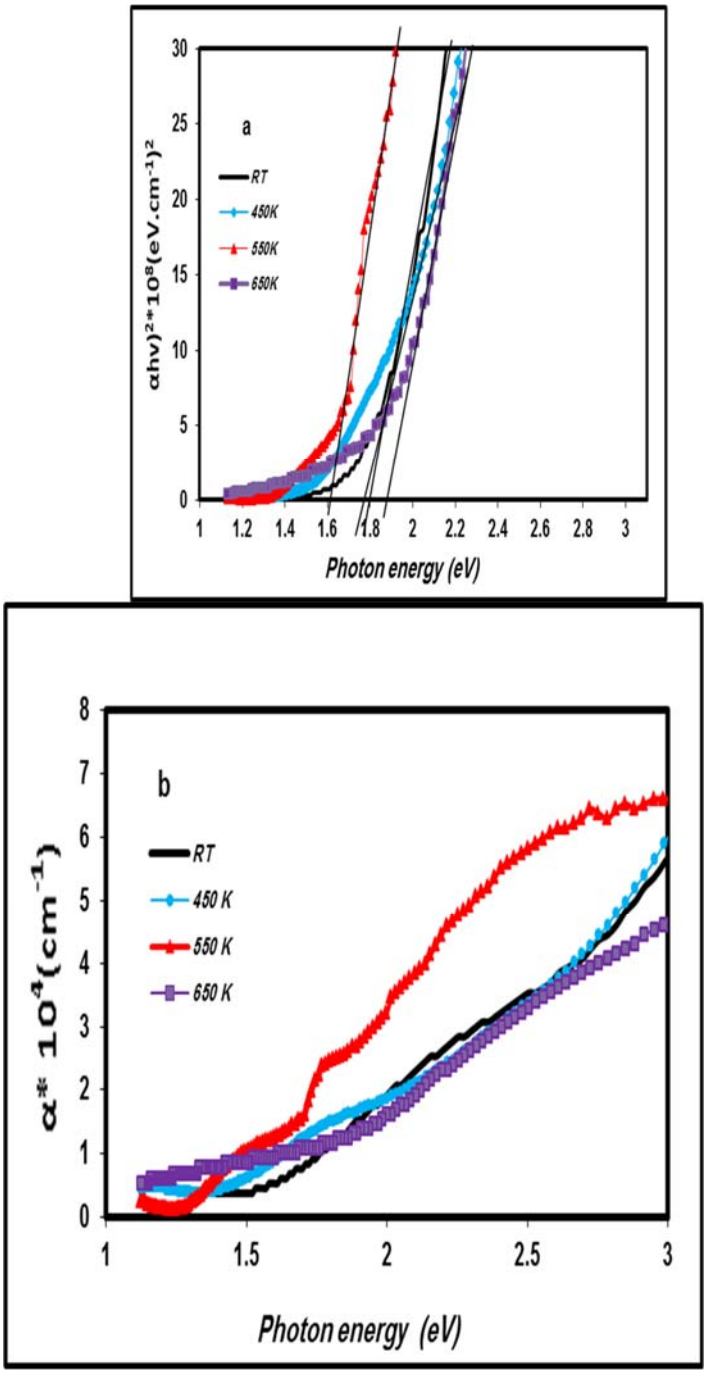

Figure (6): (a) variation $(\alpha h\upsilon)^2$ verse photon energy, (b) absorption coefficient verse photon energy for $AgInSe_2$thin films at different annealing temperatures.

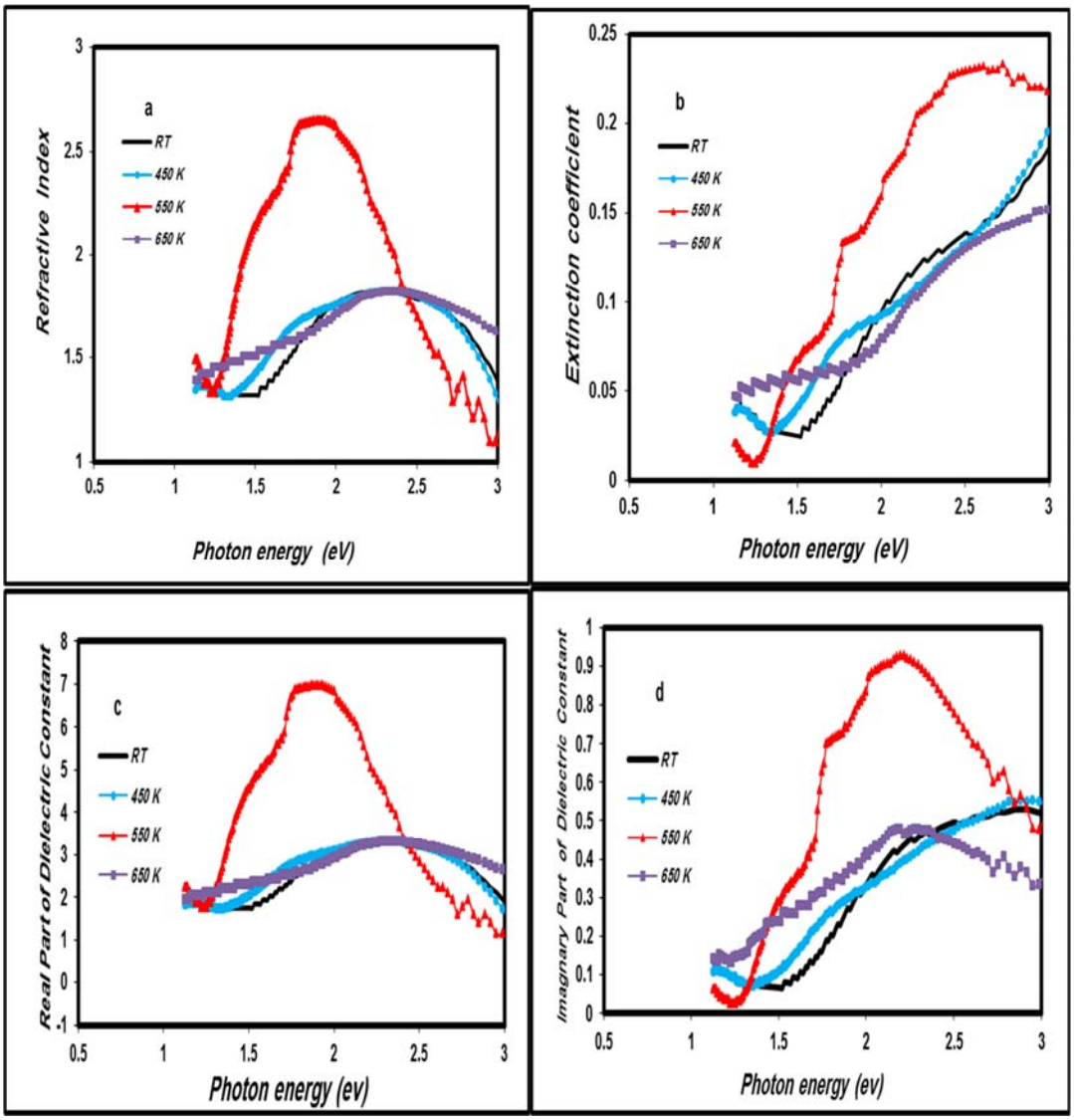

Figure (7): Variation of refractive index (a) Extinction coefficient(b) real (c) and imaginary part of dielectric constant (d) with photon energy for $AgInSe_2$ thin films at different annealing temperatures.

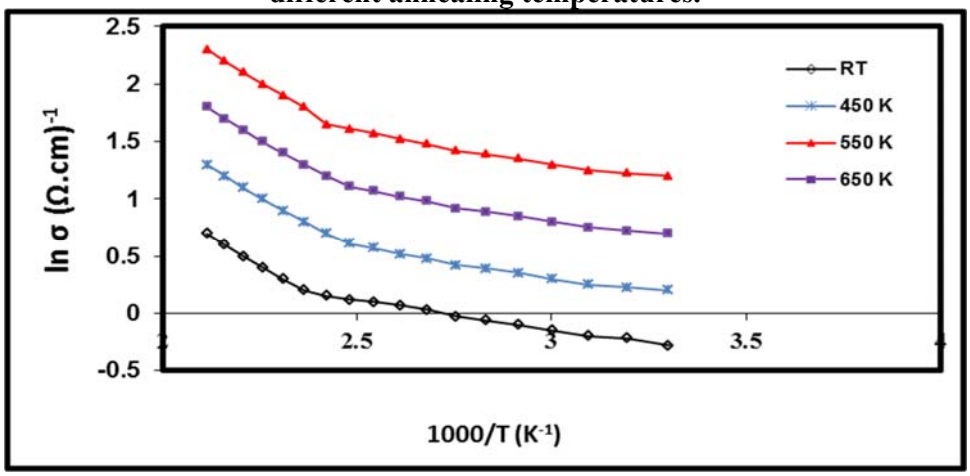

Figure (8): Ln(σ) versus reciprocal of temperature for $AgInSe_2$ films at different Ta.

Conclusions

A. $AgInSe_2$ alloy was prepared successfully and used for preparation of thin films by thermal evaporation method.
B. XRD tests for alloy and thin films showed that polycrystalline and have the tetragonal structure with preferential orientation in the [112] direction respectively.
C. The influence of annealing on the values of optical parameters of $AgInSe_2$ thin films is investigated. All thin films exhibited allowed direct optical energy band gap and high absorption in the visible region, thus, making the films suitable for optoelectronic devices, for instance as window layers of solar cells.
D.The electrical conductivity and activation energies of AIS films are seen to be dependent on the film annealing, the electrical conductivity shows as an increase of behavior with an increase of annealing. The resistivity of these films are small. Hall effect measurements confirmed that electrons were predominating in the conduction process. Both the mobility and concentration of the charge carriers increase with the increase of annealing.

References

[1]. S.Mishra, and B.Ganguli, Effect of p-d hybridization and structural distortion on the electronic properties of $AgAlM_2$ (M = S,Se,Te) chalcopyrite semiconductors, arXiv:1011.1463v1 1-15, [cond-mat.mtrl-sci] 4 Nov.(2010).
[2]. M.C. Santhosh Kumar, and B. Pradeep, Effect of H+ irradiation on the optical properties of vacuum evaporated $AgInSe_2$ thin films, Appl. Surf. Sci. 255 8324-8327, 2009.
[3]. J.J. Lee; J.D. Lee; B.Y. Ahn; H.S. Kim, and K.H. Kim, Structural and Optical Properties of $AgInSe_2$ Films Prepared on Indium Tin Oxide Substrates, J. Kor. Phys. Soc. 50, 1099-1103, (2007).
[4]. H. Mustafa; D. Hunter; A.K. Pradhan; U.N. Roy, and Y. Cui, A. Burger, Synthesis and characterization of $AgInSe_2$ for application in thin film solar cells, Thin Solid Films 515, 7001-7004.
[5]. I.V. Bodnar, Properties of AgGaxIn1 – xSe2 Solid Solutions, Inorg. Mater. 40, 914-918, (2004).
[6]. K. Yamada; N. Hoshino; T. Nakada, Crystallographic and electrical properties of wide gap $Ag(In1-x,Gax)Se_2$ thin films and solar cells, Sci. Technol. Adv. Mater. 7, 42-45, (2006).
[7]. K. Yoshino; N. Mitani; M. Sugiyama; S.F. Chichibu; H. Komaki, and T. Ikari, Optical and electrical properties of AgIn(SSe)2 crystals, Phys. B: Cond. Matter 302-303, 349-356, (2001).
[8]. J.W. Lekse; A.M. Pischera, and J.A. Aitken, understanding solid-state microwave synthesis using the diamond-like semiconductor, AgInSe2, as a case study, Mater. Res. Bull. 42 395-403, (2007).
[9]. B. D. Cullity elements of X-Ray diffraction, 2nd edition, copyright ©, by Addison – Wesley Publishing company, Inc. (1978).
[10]. D.K. Dwivedi; M.D. Vipinkumar, and H.P,Pathak, Structural, electrical and optical investigations of CdSe nanoparticles, Chalcogenide Letters, 8, 9, 521-527, (2011).
[11]. Donald A.Neamen, Semiconductor Physics and Devices, basic principles,3th edition, McGraw-Hill Companies,Inc.(2003).
[12]. J. R, Ray Panchal C.J., Desai M.S., and Trivedi U. B, Simulation of (CIGS) Thin film solar cells using AMPS-1D, J.Nano-Electron. Phys., 3, 747-754, 2011.
[13]. S.M,Sze Physics of semiconductor devices,2nded.,John Wiley and Sons, Inc. New York., (1981).
[14]. A.D.A., Buba and J.S.A Adelabu. Optical and Electrical Properties of Chemically Deposited ZnO Thin Films, The Pacific Journal of Science and Technology, 11, 429-434, (2010).

[15]. (M). Ahmed, Z.Sauli, U. Hashim and add Y. Al-Douri, Investigation of the absorption coefficient, refractive index, energy band gap, and film thickness for A $_{l0.11}$Ga $_{0.89}$N, A $_{l0.03}$Ga $_{0.97}$ N, and GaN by optical transmission method, Int. J. Nanoelectronics and Materials, 2, 189-195,(2009).
[16]. S.O, Kasap., Principles of Electronic Materials and Devices, 2nd edition, Mc Graw Hill. (2002).
[17]. Kenji Yoshino, Aya Kinoshita, Yasuhiro Hirakata, Minoru Oshima Keita Nomoto, Tsuyoshi Yoshitake , Shunji Ozaki and Tetsuo Ikari., Structural and electrical characterization of $AgInSe_2$ crystals grown by hot-press method, Journal of Physics: Conference Series 100 042042 ,pp1-4.(2008).
[18]. R.D. Tomlinson; A.E. Hill, and R.D. Pilkington, Ternary and Multinary Compounds, Proceedings of the 11th International Conference, University of Salford, 8-12 September, (1997).
[19]. S. Murugana, and K.R. Muralib, Structural, Optical, and Electrical Studies on Pulse Plated $AgInSe_2$ Films ACTA PHYSICA POLONICA A , 126,. 3, (2014).